Deactivation Kinetics of a HZSM-5 Zeolite Catalyst Treated with Alkali for the Transformation of Bio-Ethanol into Hydrocarbons

Ana G. Gayubo, Ainhoa Alonso, Beatriz Valle, Andrés T. Aguayo, and Javier Bilbao
Departamento de Ingeniería Química, Universidad del País Vasco, Apartado 644, 48080 Bilbao, Spain

DOI 10.1002/aic.12600
Published online April 22, 2011 in Wiley Online Library (wileyonlinelibrary.com).

The kinetics of deactivation by coke of a HZSM-5 zeolite catalyst in the transformation of bioethanol into hydrocarbons has been studied. To attenuate deactivation, the following treatments have been carried out: (i) the zeolite has been subjected to a treatment with alkali to reduce the acid strength of the sites and (ii) it has subsequently been agglomerated into a macro and meso-porous matrix of bentonite and alumina. The experimental study has been conducted in a fixed bed reactor under the following conditions: temperature, between 300 and 400°C; pressure, 1 atm; space-time, up to 1.53 (g of catalyst) h (g of ethanol)$^{-1}$; particle size of the catalyst, between 0.3 and 0.6 mm; feed flowrate, 0.16 cm^3 min^{-1} of ethanol+water and 30 cm^3 (NC) min^{-1} of N_2; water content in the feed, up to 75 wt %; time on stream, up to 31 h. The expression for deactivation kinetics is dependent on the concentration of hydrocarbons and water in the reaction medium (which attenuates the deactivation) and, together with the kinetics at zero time on stream, allows the calculation of the evolution with time on stream of the yields and distribution of products (ethylene, propylene and butenes, C_1-C_3 paraffins, and C_4-C_{12}). By increasing the temperature in the 300–400°C range the role of ethylene on coke deposition is more significant than that of the other hydrocarbons (propylene, butenes and C_4-C_{12}), which contribute to a greater extent to the formation of coke at 300°C.
AIChE J, 58: 526–537, 2012
Keywords: biorefinery, bioethanol, olefins, HZSM-5 zeolite, deactivation, kinetic model

Introduction

Progressive depletion of conventional fossil fuels, with increasing energy demand and greenhouse emissions have led to move toward alternative, renewable, efficient, and cost-effective energy sources with lesser emissions. Consequently, a great technological development has been reached for obtaining biofuels from biomass and between 1980 and 2005 worldwide production of biofuels (ethanol, methanol, dimethyl ether, biodiesel, Fischer-Tropsch diesel, hydrogen, methane, among others) increased by an order of magnitude (from 4.4 to 40.1 billion litres).[1,2]

Ethanol from biomass (bio-ethanol) is an attractive fuel since it can be blended with gasoline taking advantage of the higher octane number and vaporization heat.[3] Moreover, although bio-ethanol has a low cetane number and low

Correspondence concerning this article should be addressed to A. G. Gayubo at anaguadalupe.gayubo@ehu.es.

viscosity, biodiesel/bio-ethanol blends have many advantages, such as the improvement in the ability to flow under cold start conditions and the reduction in smoke and particulate material.[4] Bio-ethanol can also be used as a fuel in direct ethanol fuel cell.[5]

The major producers of bio-ethanol are Brazil (from sugar cane) and United States (from maize) which account for 70% of the world production. Second generation biofuels manufactured from lignocellulosic biomass (forest and agricultural residues, and demolition wood) partially reduces the problems associated with the valorisation from sugar containing plants, cereals crops and vegetable oils, in terms of impact in the cost of food, energy balances, green-house gas emissions, geographical diversity of production, land, and water requirement.[6] Bio-ethanol production from lignocellulosic biomass (second generation biofuel) has been greatly improved by new technologies,[7] and the perspectives for implementation in the short term are better than other biofuels (such as bio-methanol).[8] Nevertheless, to achieve the commercialization a number of technological breakthroughs and cost reductions are required, and moreover, it must be combined with the production of many high-value co-products (organic fertilizers and xylooligosaccharides) simultaneously with bio-ethanol.[9]

In addition to its use as a fuel, the bio-ethanol can be valorized by catalytic transformation by two main routes: (i) to obtain H_2 by catalytic steam reforming on a bifunctional catalyst,[10–12] and (ii) to obtain hydrocarbons. These routes have the main advantage over the use of bio-ethanol as a fuel of avoiding the costly step of water separation. The objectives of the catalytic transformation into hydrocarbons are the selective production of C_2-C_4 olefins, whose demand is growing, or the production of BTXE aromatics (benzene, toluene, xylene, and ethyl benzene), which as of interest as raw materials.[13,14]

Furthermore, the growing interest for obtaining C_2-C_4 olefins from alternative sources to petroleum, specially the production of propylene, is boosted by the limitations of the current processes for obtaining olefins at large-scale, which are the steam reforming of naphthas and the catalytic cracking (FCC), whose main feed is vacuum gasoil.[15]

The studies on the transformation of bio-ethanol into C_2-C_4 olefins have mainly been aimed in the literature at the selective production of ethylene, which is the product of bio-ethanol dehydration. Accordingly, the HZSM-5 zeolite is effective below 300°C and has been used with different modifications aimed at moderating its acid strength to avoid secondary reactions of ethylene conversion and to attenuate coke formation.[16–20] However, propylene and butene production takes place by transformation of ethylene through a oligomerization-cracking mechanism that requires temperatures above 350°C.[21–23] The main difficulty of this process is catalyst deactivation, although a distinction must be made between reversible deactivation (due to coke deposition) and the zeolite irreversible deactivation due to water content in the reaction medium (dealuminization).[24]

In a previous study, the good performance of a catalyst based on a HZSM-5 zeolite treated with 0.2 M NaOH solution for 10 min has been proven. The treatment is effective to: (i) reduce the acid strength of the sites, which attenuates coke formation; (ii) generate a mesoporous structure which reduces the external blocking of micropores by coke.[25] Subsequently, a reaction scheme and kinetic model that quantify the yields and product distribution at zero time on stream have been proposed.[26] It should be noted that this model also quantifies the attenuation of the rates of the reaction steps by the water content in the medium.

The deactivation kinetics has been studied in this article which, based on the results of the effect of operating conditions, will be dependent on the concentration of components (organics and water) in the reaction medium. In order to achieve this objective, conditions for negligible irreversible deactivation have been used.[25] Furthermore, to analyze the deactivation kinetic data, a previously developed methodology that rigorously takes into account the ''past history'' of the catalyst has been used.[27–30] The catalyst deactivation is a key factor for the economic viability of the large-scale bio-ethanol transformation process and for evaluating the possibility of co-feeding bio-ethanol into the industrially implemented MTO process (methanol to olefins) units. This opportunity is based on the similarities between the two catalytic processes over a HZSM-5 zeolite catalyst.[31]

Experimental

Catalyst

The catalyst consists of 25 wt % of active phase (HZSM-5 zeolite with $SiO_2/Al_2O_3 = 30$, treated with alkali), agglomerated by wet extrusion with bentonite as binder (30 wt %) and with alumina calcined at 1000°C as inert charge (45 wt %), to confer the catalyst high mechanical resistance for its use in a fixed or fluidized bed reactor. The zeolite is commercial (Zeolyst Int.) and supplied in ammonium form. In a previous study, the steps of the alkaline treatment (with 0.2 M NaOH solution for 10 min) of the zeolite and its agglomeration have been described in detail.[25] The physical properties of the treated HZSM-5 zeolite and of the catalyst (Table 1) were determined by N_2 adsorption-desorption (Micromeritics ASAP 2010) and by Hg porosimetry (Micromeritics Autopore 9220).

The pore volume increases slightly compared with that of the untreated zeolite as a result of the formation of mesopores, which promote accessibility to the micropores that are difficult to access in the untreated zeolite.[25] In the results of pore volume distribution, it must be taken into account that the matrix (bentonite and alumina) that dilutes the zeolite (25 wt%) provides the catalyst with all the macropores and most of the mesopores. A slight increase in the mesopore volume was also observed when comparing the images of transmission electron microscopy (TEM) (Philips CM200) for the untreated HZSM-5 zeolite and after alkaline treatment for 10 min. The expansion of the micropore outlets as a result of alkaline treatment also contributes to this increase.[25]

The total acidity (0.58 mmol of NH_3) (g of zeolite)$^{-1}$) and the acid strength distribution of the catalyst were determined by calorimetric measurement of differential adsorption of NH_3 at 150 °C and subsequent TPD of the adsorbed NH_3 with a ramp of 5°C min^{-1} up to 550°C. The equipment used was a thermobalance (SDT 2960 TA Instruments) connected online to a mass spectrometer (Thermostar of Balzers Instruments).[32,33] The alkaline treatment contributes to homogenizing the acid strength of the HZSM-5 zeolite sites to an average acidity of 125 kJ (mol of NH_3)$^{-1}$.

Table 1. Physical Properties of the Modified Zeolite and of the Catalyst

AT10-HZSM-5 zeolite				
BET Surface Area, $m^2\ g^{-1}$	Mesopore Volume, $cm^3\ g^{-1}$	Micropore Volume (*t*-plot), $cm^3\ g^{-1}$	Micropore Volume (HK), $cm^3\ g^{-1}$	Pore Diameter (HK), Å
420	0.18	0.10	0.18	5.6

Catalyst				
BET Surface Area, $m^2\ g^{-1}$	Mesopore Volume, $cm^3\ g^{-1}$	Mesopore Diameter, Å	Pore Volume Distribution (%) <20/20< d_p (Å)<500/>500	Solid Density, $g\ cm^{-3}$
193	0.61	186	5.1/39.9/55.0	1.79

Equipment and reaction conditions

The kinetic runs have been carried out in an automated device equipped with an isothermal fixed bed reactor (of 316 stainless steel with 9 mm of internal diameter and 10 cm of total effective length). At the reactor outlet, the reaction products pass through a six-way valve that sends the reaction product sample to a chromatograph (Hewlett Packard 6890 Series II) and to a micro-GC (Varian CP). The operating conditions are controlled by a software specifically designed for this process called Adkir.[26]

The data for the kinetic modeling have been obtained under the following operating conditions: temperature, between 300 and 400°C; pressure, 1 atm; space-time, up to 1.53 (g of catalyst) h (g of ethanol)$^{-1}$; particle size of the catalyst, between 0.3 and 0.6 mm; feed flow-rate, 0.16 $cm^3\ min^{-1}$ of ethanol+-water and 30 cm^3 (NC) min^{-1} of N_2; water content in the feed, up to 75 wt %; time on stream, up to 31 h. Apart from the runs at constant temperature, additional ones have been carried following a sequence of temperature-time on stream to study the effect of operating conditions on deactivation and experimentally verify the kinetic model.

Results

Kinetics at zero time on stream

The kinetics at zero time on stream was studied in a previous paper, in which the scheme of lumps shown in Figure 1 was established based on kinetic data at zero time on stream.[26] The reaction products were grouped into four lumps: (i) ethylene, which is really the reactant because ethanol dehydration is very fast under the conditions studied; (ii) light olefins (propylene and butenes), which commercially are the most interesting products; (iii) components in the C_4–C_{12} range (briefly denoted lump of gasoline), comprising C_{4+} paraffins, C_{5+} olefins and aromatics; (iv) light paraffins (methane, ethane and propane). The kinetic equations for the scheme in Figure 1 are:[26]

$$(-r_E)_0 = \{[k_1 + k_5 + (k_2 + k_4)X_O]X_E - k_6X_G\} \cdot \theta \quad (1)$$

$$(r_O)_0 = [k_1X_E + (k_2 - k_4)X_OX_E - k_3X_O + k_6X_G] \cdot \theta \quad (2)$$

$$(r_G)_0 = (k_3X_O + 2k_4X_EX_O - 3k_6X_G) \cdot \theta \quad (3)$$

$$(r_P)_0 = (k_5X_E + k_6X_G) \cdot \theta \quad (4)$$

In Eqs. 1–4, the concentration of each lump, X_i, is defined as the mass fraction by mass unit of organic compounds in the reaction medium (excluding water). The term θ quantifies the attenuation of the kinetic steps by the water content in the reaction medium. It has been determined by the expression:

$$\theta(X_W) = \exp(-K_WX_W) \quad (5)$$

where K_W constant is related to temperature according to the expression:

$$K_W = K_W^* \exp\left[-\frac{E_W}{R}\left(\frac{1}{T} - \frac{1}{573}\right)\right] \quad (6)$$

In Eq. 6, K_W^* is the value corresponding to the reference temperature, 300°C.

It should be noted that ethanol dehydration step was not considered in the kinetic model, because this reaction is instantaneous under the conditions studied and ethylene is the true reactant for the formation of other hydrocarbons.

The values of activation energies and kinetic constants in Eqs. 1–4 and 6 are shown in Table 2 for a reference temperature (300°C).[26]

Effect of reaction conditions on deactivation

Figure 2 shows the results of the evolution with time on stream of lump concentrations in the product stream. The results in Figure 2a correspond to the water content for an azeotropic mixture in the feed (5 wt%), which limits the atmospheric distillation, and two temperatures (350 and 375°C). The results in Figure 2b correspond to a given temperature (350°C) and two water contents in the feed (5 and 75 wt %). The results satisfy the following conditions: (1) the concentration of hydrocarbons in the reaction medium is similar in each graph, so that the effect of the composition does not mask the effect of temperature (Figure 2a) and of water concentration (Figure 2b) on deactivation; (2) the deactivation of the catalyst takes place only by coke and the irreversible deactivation of the zeolite by dealuminization is

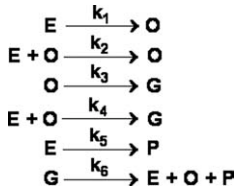

Figure 1. Kinetic scheme for bio-ethanol transformation.[26]

Table 2. Kinetic Parameters (Kinetic Constants at 300°C, Activation Energies and Parameter for Attenuation due to Water) of the Kinetic Model (Eqs. 1–6) for Bio-ethanol Transformation at Zero Time on Stream[26]

Parameter		
k_1, $g_{EtOH}\ (g_{cat})^{-1}\ h^{-1}$	0.626	± 0.052
k_2, $g_{EtOH}\ (g_{cat})^{-1}\ h^{-1}$	6.208	± 0.517
k_3, $g_{EtOH}\ (g_{cat})^{-1}\ h^{-1}$	2.068	± 0.230
k_4, $g_{EtOH}\ (g_{cat})^{-1}\ h^{-1}$	6.042	± 0.731
k_5, $g_{EtOH}\ (g_{cat})^{-1}\ h^{-1}$	0.018	± 0.003
k_6, $g_{EtOH}\ (g_{cat})^{-1}\ h^{-1}$	0.016	± 0.003
K_w	0.230	± 0.007
E_1, kJ mol^{-1}	96.85	± 3.13
E_2, kJ mol^{-1}	70.60	± 3.97
E_3, kJ mol^{-1}	54.43	± 4.22
E_4, kJ mol^{-1}	59.81	± 4.64
E_5, kJ mol^{-1}	148.3	± 7.52
E_6, kJ mol^{-1}	130.4	± 6.23
E_w, kJ mol^{-1}	24.35	± 1.21

negligible, which has been proven by reaction-regeneration cycles in which the catalyst maintains its performance.[25]

Figure 2 shows that, as a result of the deactivation by coke, ethylene concentration increases with time on stream, whereas the concentration of other hydrocarbons decreases (or remains almost constant in the case of propylene + butenes lump). It is clear that deactivation increases with temperature, whereas an increase in water content in the reaction medium attenuates deactivation. Therefore the presence of water has an unfavorable effect of attenuating the reaction rates of the kinetic steps, quantified with the term θ in Eqs. 1–4, and a favorable effect of attenuating the deactivation by coke. This fact has been previously observed for the transformation of bio-ethanol into hydrocarbons,[22,24,34] and it is a key factor for controlling the deactivation in the transformation of other oxygenates into hydrocarbons, such as methanol and the bio-oil obtained from pyrolysis of lignocellulosic biomass.[35–37] The moderation of the acid strength of the sites caused by hydration and the competition of water with hydrocarbons (coke precursors in the deactivation) in their adsorption on the acid sites explain the attenuation in the reaction rates of the steps caused by water.[34,36]

Methodology for kinetic modeling

The methodology used for the kinetic modelling of deactivation is summarized by the following steps: (i) proposal of alternative kinetic models (ii) solving each model and calculation of the corresponding kinetic parameters, (iii) discrimination of models.

The calculation of the parameters of a deactivation kinetic model requires to solve simultaneously the partial differential equations corresponding to the mass balances for the lumps involved in the kinetic scheme (Figure 1) and the deactivation kinetic equation that quantifies the effect of operating conditions (time on stream, temperature, and components concentration) on activity. Thereby, the past history of the catalyst at each position of the reactor is taken into account, which is necessary when the deactivation is dependent on the composition of the reaction medium.[27–30]

The mass conservation equation for each i lump in the scheme in Figure 1 is established considering plug flow for the fixed bed reactor. Expressing the longitudinal coordinate as dimensionless, ξ, and with the concentrations defined as mass fraction my mass unit of organic components, the equation is:

$$\frac{\partial X_i}{\partial t} = \frac{(1-\varepsilon)\rho}{\varepsilon}\frac{RT}{P\overline{M}}(r_i)_0\left(\frac{m_0}{F_{E0}}\right)a - \frac{u}{Z}\frac{\partial Xi}{\partial \xi} \tag{7}$$

where the activity, a, is defined as the ratio between the reaction rates at t time on stream and zero time on stream:

$$a = \frac{r_i}{(r_i)_0} \tag{8}$$

The ethylene transformation rate and the formation rate of each lump of products at zero time on stream ($(r_i)_0$ in Eqs. 7 and 8), corresponds to Eqs. 1–4, with the kinetic parameters in Table 2.

To solve Eq. 7, the following boundary conditions at the reactor inlet are considered:

$$X_i(\xi = 0, t) = X_{i0} \tag{9}$$

$$a(\xi = 0, t) = a(X_{i0}, t) \tag{10}$$

and the initial conditions:

$$X_i(\xi, t = 0) = X_{i0}(\xi) \tag{11}$$

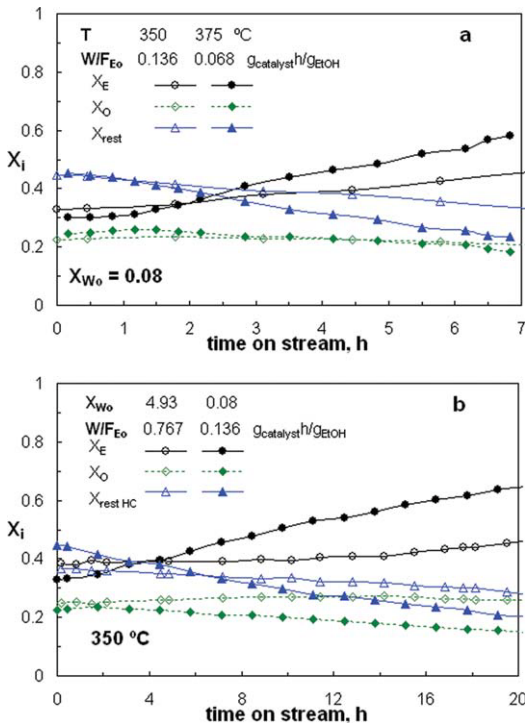

Figure 2. Evolution with time on stream of the concentration of products, for two temperatures (Graph a) and two water contents in the feed (Graph b).

[Color figure can be viewed in the online issue, which is available at wileyonlinelibrary.com].

$$a(\xi, t=0) = 1 \tag{12}$$

The concentration profile across the bed at zero time on stream, $X_{i0}(\xi)$, is calculated by solving the mass conservation equation under these conditions (without the accumulation term in Eq. 7 and with $a = 1$):

$$\frac{dX_i}{d\xi} = \frac{Z(1-\varepsilon)\rho}{F_{E0}} \frac{RT}{PM} \frac{m}{u\varepsilon} (r_i)_0 = \frac{Z(1-\varepsilon)\rho S}{F_{E0}} (r_i)0 \tag{13}$$

The kinetic constants of best fit to the experimental results for each deactivation kinetic model proposed are those that minimize an error objective function, Φ, defined as the sum of square errors between the experimental and calculated values of concentration:

$$\Phi = \sum_{i=1}^{n_1} \sum_{j=1}^{n_{exp}} \left(X^*_{i,j} - X_{i,j} \right)^2 \tag{14}$$

where: $X^*_{i,j}$ is the experimental concentration of i lump for the experimental condition j; $X_{i,j}$ is the corresponding calculated value; n_l is the number of lumps in the kinetic scheme; n_{exp} is the total number of experimental conditions. The models tested are for "non-selective" deactivation, because they consider the same deactivation kinetics for all the steps in the kinetic scheme in Figure 1. Consequently, weight factors for the different lumps are not considered in the calculation of Eq. 14.

A calculation program written in Matlab has been used for integrating the mass balances and minimizing the error objective function. This code sequentially uses firstly an algorithm based on Levenberg-Marquardt method and then the *fminsearch* algorithm provided by Matlab.

The discrimination between deactivation kinetic models has been based on the F test of significance between the values of lack of fit variances for pairs of models. Thus, if the fit of j model is significantly better than that of i model, the statistic calculated as the ratio of their lack of fit variances will be:

$$\frac{(s^2_f)_i}{(s^2_f)j} > F_\alpha \left[(\nu_f)_i, (\nu_f)_j \right] \tag{15}$$

Discrimination of deactivation kinetic models

It has been considered that the only cause of deactivation is coke deposition, since the irreversible deactivation (by dealuminization of the zeolite) is negligible in the range of operating conditions used.[25] The kinetic equation of deactivation should take into account the effect of temperature and of concentration of coke precursor species. Furthermore, the attenuating effect of water must also be considered. The general expression adopted for the deactivation kinetics is:

$$-\frac{da}{dt} = -\sum_i k'_{di} X_i a^{nd} \tag{16}$$

where X_i is the concentration of each lump that is coke formation precursor, n_d is the order of deactivation and k'_{di} is the apparent kinetic constant of deactivation for each coke precursor. This constant is defined as the product of the corresponding kinetic constant of deactivation, k_{di}, and a deactivation attenuating function, $\theta_d(X_W)$, dependent on water content in the reaction medium:

$$k'_{di} = k_{di} \theta_d(X_W) \tag{17}$$

Table 3. Expressions Studied for the Kinetic Equation of Deactivation

Model No	Equation	
1	$\frac{da}{dt} = -k_d a^{n_d} \theta_d$	(20)
2	$\frac{da}{dt} = -k_d X_E a^{n_d} \theta_d$	(21)
3	$\frac{da}{dt} = -k_d X_G a^{n_d} \theta_d$	(22)
4	$\frac{da}{dt} = -k_d (X_O + X_G) a^{n_d} \theta_d$	(23)
5	$\frac{da}{dt} = -(k_{d1} X_O + k_{d2} X_G) a^{n_d} \theta_d$	(24)
6	$\frac{da}{dt} = -[k_{d1} X_E + k_{d2} (X_O + X_G)] a^{n_d} \theta_d$	(25)
7	$\frac{da}{dt} = -(k_{d1} X_E + k_{d2} X_O + k_{d3} X_G) a^{n_d} \theta_d$	(26)

The establishment of coke precursors in Eq. 16 encounters the difficulty of an unknown mechanism for coke formation. Although coke formation in the transformation of methanol upon HZSM-5 zeolite catalysts is related to the generation of polymethylbenzenes (trimethyl-and tetramethyl benzene),[38] the compounds retained within the zeolite in the transformation of ethanol are not polymethylbenzenes but ethyl methyl benzenes.[39] Furthermore, the deactivation in the transformation of methanol is dependent on the concentration of oxygenates (methanol and dimethyl ether) in the reaction medium, which activate the hydrocarbon pool mechanism.[40–42] Nevertheless, the dehydration of bio-ethanol is very rapid and complete at the reactor inlet section, so that ethylene is the real reactant and its transformation into higher hydrocarbons takes place mainly through oligomerization-cracking mechanism,[43] with secondary reactions of mainly hydrogen transfer. These secondary reactions are likely to be important in the formation of coke.

Given the uncertainty concerning the dependence of deactivation on component concentration in the reaction medium, different expressions have been assayed for the kinetic equation of deactivation (Table 3): (i) independent of reaction medium concentration (model 1), (ii) dependent on the concentration of ethylene (deactivation in parallel with the main reaction, Model 2), (iii) dependent on the concentration of gasoline lump, Model 3; (iv) dependent on the concentrations of olefin and gasoline lumps, with one kinetic parameter (Model 4) or two parameters (Model 5); (v) dependent on the concentration of ethylene and other hydrocarbons (Model 6) or considering separately the effect of the concentration of each lump of hydrocarbons (Model 7). In all cases, the fitting results show the need for incorporating a term, θ_d, that quantifies the attenuating effect of water into the deactivation kinetic equation (by multiplying the kinetic constant),

Table 4. Kinetic Parameters for the Deactivation Kinetic Equations (Kinetic Models 1–7 in Table 3) and Parameters for Significance Test

Parameters	Model 1	Model 2	Model 3	Model 4	Model 5	Model 6	Model 7
k_d, h^{-1}	0.024 ± 0.001	0.076 ± 0.001	0.181 ± 0.021	0.161 ± 0.017	–	–	–
k_{d1}, h^{-1}	–	–	–	–	0.179 ± 0.017	0.015 ± 0.001	0.016 ± 0.001
k_{d2}, h^{-1}	–	–	–	–	0.044 ± 0.005	0.032 ± 0.002	0.033 ± 0.002
k_{d3}, h^{-1}	–	–	–	–	–	–	0.032 ± 0.003
K_{dW}	0.361 ± 0.030	0.242 ± 0.007	0.337 ± 0.054	0.204 ± 0.029	0.324 ± 0.037	0.238 ± 0.023	0.231 ± 0.025
E_d, kJ mol^{-1}	74.70 ± 2.17	10.27 ± 0.63	53.25 ± 4.60	34.54 ± 4.05	–	–	–
E_{d1}, kJ mol^{-1}	–	–	–	–	76.91 ± 3.76	98.69 ± 2.51	97.06 ± 2.38
E_{d2}, kJ mol^{-1}	–	–	–	–	25.24 ± 1.46	39.58 ± 0.990	39.51 ± 1.01
E_{d3}, kJ mol^{-1}	–	–	–	–	–	–	37.18 ± 1.73
E_{dW}, kJ mol^{-1}	8.941 ± 0.30	18.72 ± 1.35	5.060 ± 0.56	21.65 ± 3.69	18.87 ± 2.27	14.54 ± 0.744	14.76 ± 1.49
n_d	1.919 ± 0.103	1.275 ± 0.023	2.073 ± 0.180	2.093 ± 0.150	2.504 ± 0.124	1.845 ± 0.077	1.756 ± 0.066
Φ	2.297	4.297	3.579	3.443	2.556	2.101	2.085
s_f^2	$1.485\ 10^{-3}$	$2.778\ 10^{-3}$	$2.313\ 10^{-3}$	$2.225\ 10^{-3}$	$1.654\ 10^{-3}$	$1.360\ 10^{-3}$	$1.351\ 10^{-3}$
SS_E	0.883	1.980	1.725	1.661	1.072	0.823	0.812
SS_O	0.391	0.506	0.546	0.539	0.449	0.374	0.374
SS_G	0.815	1.606	1.129	1.059	0.871	0.734	0.731
SS_P	0.166	0.205	0.179	0.183	0.165	0.169	0.167

which is dependent on water content in the reaction medium, X_W (expressed by mass unit of organic components). Different expressions have been tested (exponential, potential, hyperbolic) to relate θ_d with X_W but, for the sake of simplicity, the results shown below correspond only to an exponential expression of $\theta_d(X_W)$ function, which is that of best fit:

$$\theta_d(X_W) = \exp(-K_{dW}X_W) \tag{18}$$

Likewise, we have omitted results corresponding to expressions of the deactivation kinetic equation that consider light paraffins (C_1–C_3) as possible precursors of coke, since its role in deactivation has been proven to be insignificant.

The sum of water co-fed with ethanol, X_{W0}, plus that formed by ethanol dehydration, X_{Wf}, are considered in the calculation of X_W. Under the experimental conditions used in this study (which correspond to total dehydration of ethanol into ethylene):

$$X_{Wf} = \frac{18}{28}\left(\frac{g_{H_2O}/mol_{EtOH}}{g_{C2=}/mol_{EtOH}}\right) = 0.643\left(\frac{g_{H_2O}}{g_{C2=}\text{in the feed}}\right) \tag{19}$$

Table 4 shows the kinetic parameters with a 95% confidence interval and the values for significance testing statistical factors (objective function, variance for the lack of fit and the sum of squared errors for each lump) corresponding to the best fit for the deactivation kinetic equations shown in Table 3. The values of the kinetic parameters at zero time on stream (Table 2),[26] have been adopted as fixed values in all the fittings.

Based on the results in Table 4, the best fit corresponds to the models of deactivation that consider ethylene and C_3–C_4 olefins and gasoline (C_4–C_{12}) as coke precursors (models 6 and 7). Table 5 shows the results of significance test for model 7 compared with the other models. There are 388 experimental conditions (without repetitions) so that the degrees of freedom for model 7 are $\nu_{M7} = 1543$. It should be noted that model 7 is significantly better than Models 1–5 but not than Model 6.

To illustrate the model's adequacy for predicting the kinetic results of deactivation, Figures 3 and 4 compare the experimental results of the evolution of ethylene concentration with time on stream (points) with the values calculated using four of the models assayed (lines), and Figure 5 compares the corresponding experimental and calculated results of the evolution of ethylene and gasoline lump concentrations with time on stream. For the sake of simplicity, the results for Model 7 are not shown in Figures 3–5, given that their fit to the experimental results is similarly to Model 6 due to the very close values of k_{d3} and k_{d2} kinetic constants for this Model 7. Consequently, the curves corresponding to Model 7 (not plotted) almost overlap those for Model 6.

Figure 3 corresponds to experiments in which a temperature-time sequence has initially been established and then the temperature was maintained for a given period. The results correspond to two different values of space time for a feed with 5 wt % water. Figure 4 corresponds to the experiments at constant temperature (350°C) for two different

Table 5. Significance Test Results for Model 7 with the Remaining Deactivation Kinetic Models in Table 3

Parameters	Model 1	Model 2	Model 3	Model 4	Model 5	Model 6
$\left(s_f^2\right)_i \Big/ \left(s_f^2\right)_7$	1.099	2.056	1.712	1.647	1.224	1.007
$(\nu_f)_i$	1547	1547	1547	1547	1545	1545
$F_{0.05}[(\nu_f)_i,(\nu_f)_7]$	1.087	1.087	1.087	1.087	1.087	1.087
Significant improvement?	Yes	Yes	Yes	Yes	Yes	No

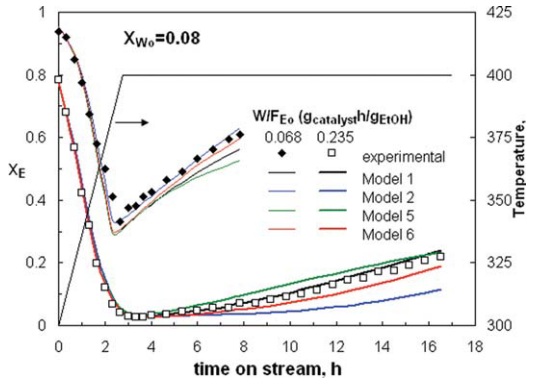

Figure 3. Comparison of the fit between the results calculated (lines) using different deactivation kinetic models (Models 1, 2, 5, and 6 in Table 2) and the experimental results (points) of evolution with time on stream of ethylene concentration in the product stream.

Experimentation with a ramp of temperature-time and a feed with 5 wt % water. [Color figure can be viewed in the online issue, which is available at wileyonlinelibrary.com].

water contents in the feed (5 wt %, Graph a, and 50 wt %, Graph b) and different space times. The results in Figures 3 and 4 correspond to conditions under which the deactivation is slow and, consequently, there are no very noticeable differences between the results calculated with the different kinetic models.

Nevertheless, the differences between the predictions of the models are significant under conditions with fast deactivation. These conditions are those of Figure 5, which correspond to the highest temperature in the range studied (400°C) and the water content in the feed corresponds to the bio-ethanol azeotrope, 5 wt %). The conversion of ethylene is high at zero time on stream and, therefore, there is a significant concentration of olefin and gasoline lumps. Under these conditions of rapid deactivation, the best fit of Model 6 to the experimental results of evolution with time on stream of ethylene and gasoline lump concentration in the product stream is clearly shown.

Kinetic model proposed

Based on the aforementioned results for fitting the different kinetic models to the experimental results of deactivation in the 300–400°C range, Model 6 in Table 3 (Eq. 25) is the most suitable, given that it strikes the best balance between fitting quality and simplicity. Analyzing the values of the kinetic parameters for this model, the value of the constant that quantifies the contribution of products (olefins and gasoline lump) to the formation of coke at the reference temperature of 300°C, $k_{d2} = 0.032\ h^{-1}$, is twice the value of the constant for ethylene, $k_{d1} = 0.015\ h^{-1}$. However, since the activation energy for ethylene constant, E_{d1}, is greater than that for the other lumps of olefins and gasoline (E_{d2}), the contribution of ethylene to coke formation becomes more significant as temperature is increased.

Consequently, the kinetic results of deactivation in the 300–400°C range are consistent with a mechanism of coke formation (mainly from olefins) by the well-established mechanisms of oligomerization, aromatic formation, and their condensation.[44] Ethylene oligomerization rate will presumably be more favored than that of propylene and butenes by an increase in temperature, as has already been reported in the literature.[43]

In addition to the reaction conditions, acid structure and pore morphology of the catalyst have a notable role on coke deposition. The uniform acidity of the HZSM-5 zeolite, without very strong acid sites, and its microporous structure, which is three-dimensional and without intersections, are appropriate features to minimize the formation of coke in the reactions of transformation of alcohols into hydrocarbons.[45] The catalyst used in this study has these aforementioned features.[25] First, the alkaline treatment has eliminated the strong acid sites of the HZSM-5, which have higher activity in the reactions of coke evolution.[46] Second, the

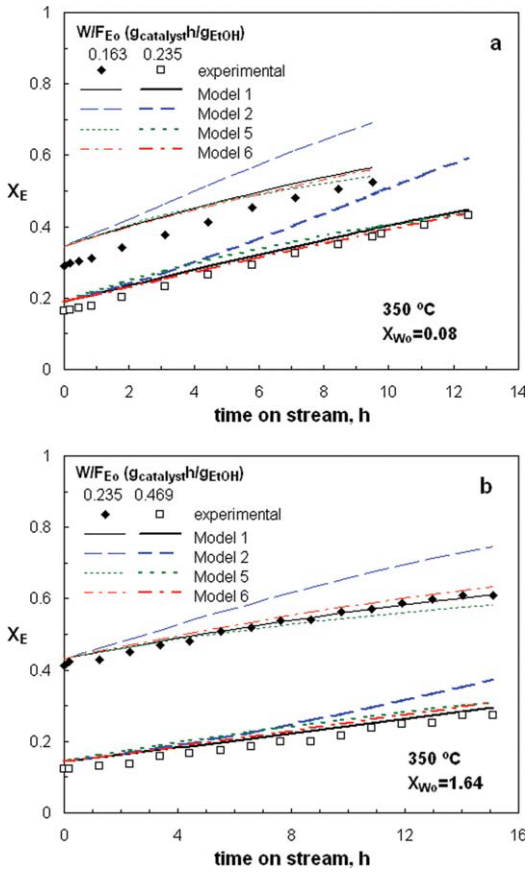

Figure 4. Comparison of the fit between the results calculated (lines) using different deactivation kinetic models (Models 1, 2, 5, and 6 in Table 2) and the experimental results (points) of evolution with time on stream of ethylene concentration in the product stream at 350°C. Graph a, X_{W0} = 0.08. Graph b, X_{W0} = 1.64.

[Color figure can be viewed in the online issue, which is available at wileyonlinelibrary.com].

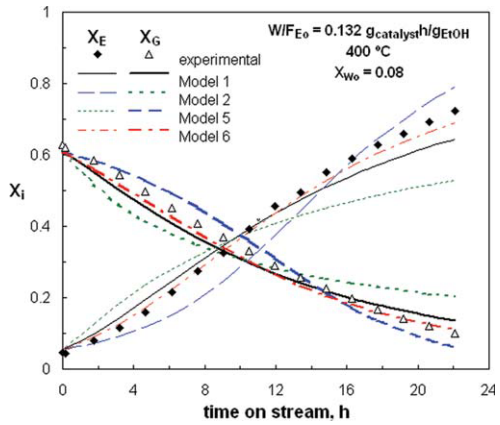

Figure 5. Comparison of the fit between the results calculated (lines) using different deactivation kinetic models (Models 1, 2, 5, and 6 in Table 2) and the experimental results (points) of evolution with time on stream of ethylene and gasoline lump concentration in the product stream at 400°C, X_{W0} = 0.08 and W/F_{E0} = 0.132 (g of catalyst) h (g of ethanol)$^{-1}$.

[Color figure can be viewed in the online issue, which is available at wileyonlinelibrary.com].

catalyst has a matrix with mesoporous structure, which facilitates the movement of coke precursors towards the outside of the crystals.[47] The agglomeration of the zeolite with bentonite and alumina generates mesopores that work as ''vessels'' of the coke dragged outside the zeolite crystalline channels, which minimizes the external blockage of the micropores.

The kinetic model established consists of: (i) the kinetic equations for the steps of the reaction scheme (Figure 1), described by Eqs. 1–4 and Eq. 5 (to quantify the attenuation due to water) and with the values of the kinetic parameters shown in Table 2;[26] (ii) the deactivation kinetic equation, Eq. 25, and Eq. 18 (to quantify the attenuation of coke deposition due to water), with the values of the kinetic parameters shown in Table 4.

To show the validity of the kinetic model in the wide range of operating conditions studied, Figures 6–8 compare the experimental values (points) of evolution with time on stream of the different lump concentration with the values calculated with the kinetic model (lines). Each figure corresponds to a value of water content in the feed: 5 wt % (X_{W0} = 0.08), 50 wt % (X_{W0} = 1.64) and 75 wt % (X_{W0} = 4.93). The reactor operates at constant temperature in all cases and the results correspond to conditions chosen as an example for both slow and rapid deactivation.

The experimental results (points) and those calculated (lines) are also compared in Figures 9–11, but in this case, a temperature-time on stream ramp of 6°C min^{-1} has initially been followed and then temperature has been maintained for a given time on stream.

A good fit between calculated and experimental results is observed for both series of experiments.

Conclusions

The catalyst prepared with the HZSM-5 zeolite treated with alkali shows a moderate deactivation by coke

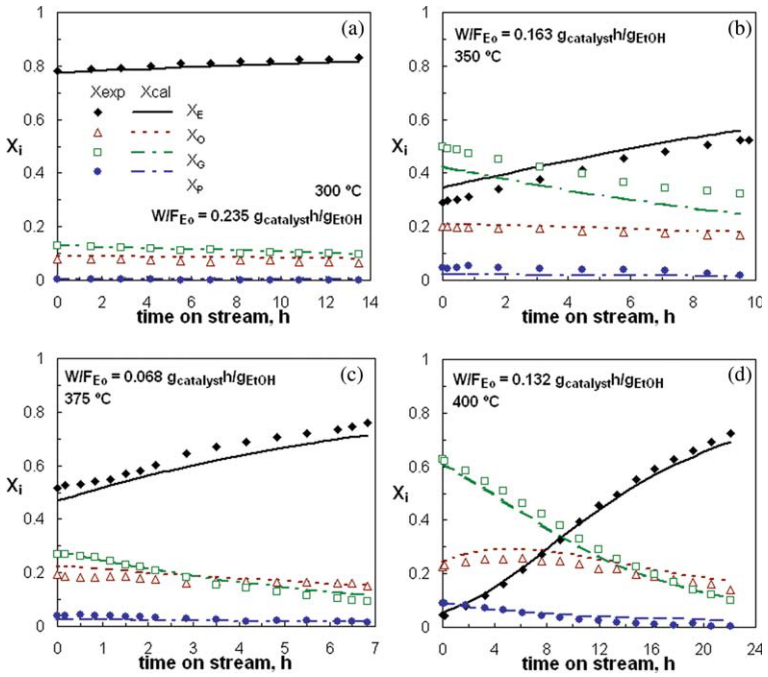

Figure 6. Analysis of the overall kinetic model proposed.

Evolution with time on stream of experimental (points) and calculated (lines) concentration of products for different temperatures and space times and 5 wt % of water in the feed. [Color figure can be viewed in the online issue, which is available at wileyonlinelibrary.com].

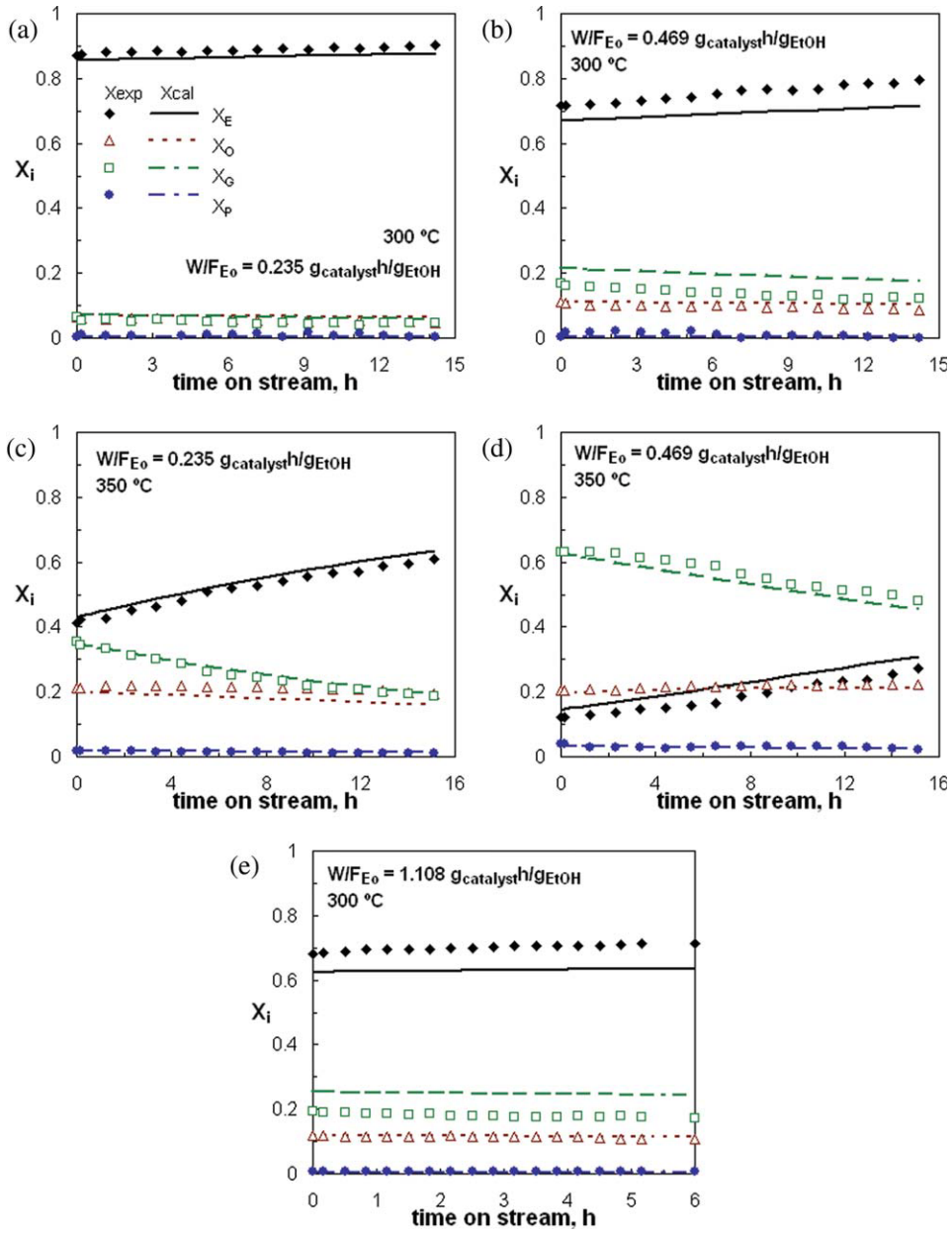

Figure 7. Analysis of the overall kinetic model proposed.

Evolution with time on stream of experimental (points) and calculated (lines) concentration of products for different temperatures and space times and 50 wt % of water in the feed. [Color figure can be viewed in the online issue, which is available at wileyonlinelibrary.com].

deposition in the 300–400°C range, as a result of its moderate acid strength and the presence of mesopores. The deactivation is favored by increasing temperature and it is attenuated by increasing water content in the bioethanol fed. This advantage of the water content in the feed is an interesting result for the viability of bio-ethanol (with a high water content) transformation process into hydrocarbons. Moreover, in addition to a similar kinetic scheme and operating conditions, this is another common feature with the MTO process, which is especially interesting from the perspective of co-feeding bio-ethanol with methanol in the MTO process for obtaining C_2–C_4 olefins with high selectivity of propylene.

The kinetic equation of deactivation determined in this work, which is dependent on the concentration of the components in the reaction medium, shows that coke formation precursors are ethylene and components of the lumps of olefins (propylene and butenes) and gasoline. It can be concluded that all the olefins play an important role in the formation of coke by oligomerization and condensation mechanisms, although the relative importance of each olefin concentration depends on temperature. By increasing temperature in

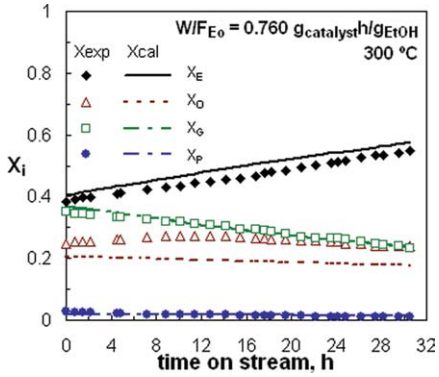

Figure 8. Analysis of the overall kinetic model proposed.

Evolution with time on stream of experimental (points) and calculated (lines) concentration of products for different temperatures and space times and 75 wt % of water in the feed. [Color figure can be viewed in the online issue, which is available at wileyonlinelibrary.com].

the 300–400°C range, the role of ethylene in coke formation is higher than that of heavier olefins.

The deactivation kinetic equation deduced in this article together with the kinetic model at zero time on stream, allows quantifying product yields and distributions in a wide range of operating conditions. The overall kinetic model

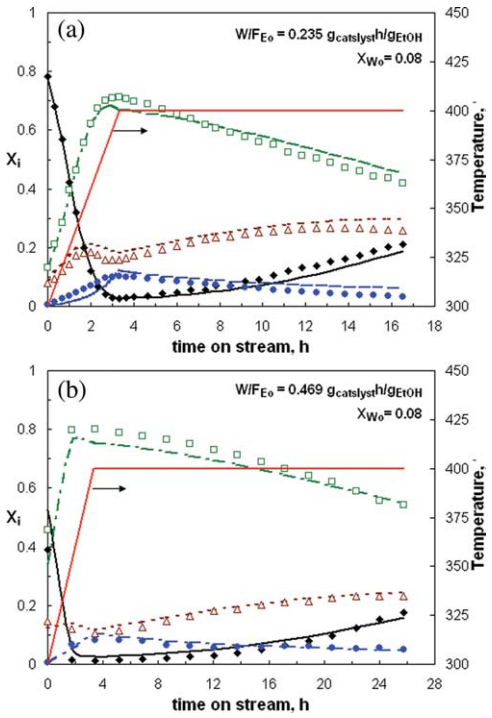

Figure 9. Analysis of the overall kinetic model proposed.

Evolution with time on stream of experimental (points) and calculated (lines) concentration of products in dynamic experiments for different space times and 5 wt % of water in the feed. [Color figure can be viewed in the online issue, which is available at wileyonlinelibrary.com].

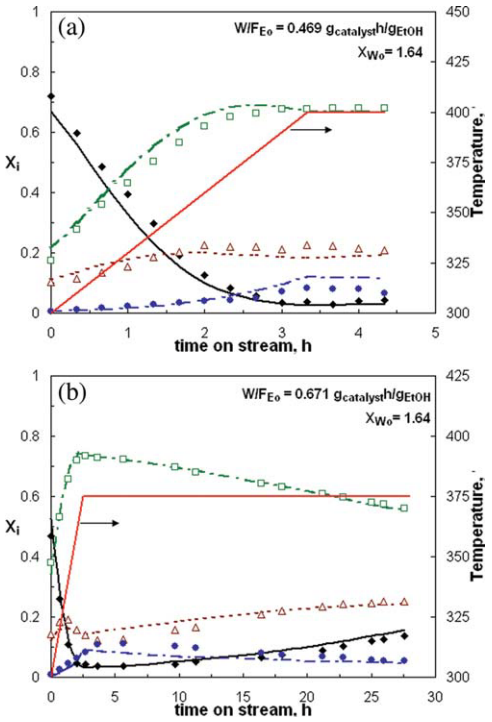

Figure 10. Analysis of the overall kinetic model proposed.

Evolution with time on stream of experimental (points) and calculated (lines) concentration of products in dynamic experiments for different space times and 50 wt % of water in the feed. [Color figure can be viewed in the online issue, which is available at wileyonlinelibrary.com].

quantifies the effect of water content in the reaction medium, which, on the one hand, attenuates the reaction rate of the main reaction steps (adverse effect) and, on the other hand, attenuates the deactivation by coke deposition (positive effect). This fact is interesting to establish the operating conditions that allow maximize the yield of commercially important products, such as propylene and butenes.

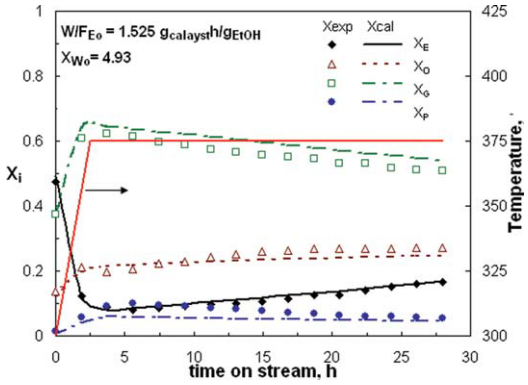

Figure 11. Analysis of the overall kinetic model proposed.

Evolution with time on stream of experimental (points) and calculated (lines) concentration of products in a dynamic experiment for $W/F_{E0} = 1.525$ (g of catalyst) h (g ethanol)$^{-1}$ and 75 wt % of water in the feed. [Color figure can be viewed in the online issue, which is available at wileyonlinelibrary.com].

Acknowledgments

This work was carried out with the financial support of the Department of Education Universities and Research of the Basque Government (Project GIC07/24-IT-220-07) and of the Ministry of Science and Innovation of the Spanish Government (Project CTQ2006-12006/PPQ).

Notation

a = activity, Eq. 8
E, G, O, P = ethylene, lump of gasoline (butane and C_{5+}), lump of propylene + butenes, and lump of light paraffins (C_{4-}), respectively
E_j, E_W = activation energy of j step in the kinetic scheme and parameter in the expression that relates K_W parameter to temperature, kJ (mol)$^{-1}$
E_{di}, E_{dW} = activation energy of kinetic constant for deactivation by the coke formed from i component, and parameter in the expression that relates K_{dW} parameter to temperature, kJ (mol)$^{-1}$
F_α = critical value of Fischer's F distribution for one-sided $100(1-\alpha)$ confidence interval
F_{E0} = mass flow rate of ethanol in the feed, g h^{-1}
k_{di} = kinetic constant for deactivation by the coke formed from i component, h^{-1}
k_j = kinetic constant of j step in the kinetic scheme, (g of ethanol) (g of catalyst)$^{-1}$ h^{-1}
K_W, K_{dW} = parameter that quantifies the resistance to formation of i component in the corresponding reaction step and the formation of coke, respectively, due to the presence of water in the reaction medium, dimensionless
$\overline{M}$ = average molecular weight of organic components, kg mol^{-1}
m_0 = mass flow rate of organic components, g h^{-1}
n_d = exponent in Eq. 16
n_{exp}, n_l = total number of experimental conditions and number of lumps in the kinetic scheme (number of dependent variables in the fitting), respectively
P = partial pressure of organic components, Pa
R = constant of gases, kJ mol^{-1} K^{-1}
$(r_i)_0$, r_i = rate of formation of i component at zero time on stream and at any time on stream, (g of i component) (g of ethanol) h^{-1} (g of catalyst)$^{-1}$ (g of organic components)$^{-1}$
S = cross sectional area of the reactor, m^2
SS_i = sum of squares for lump i
$(s_f^2)_i$ = variance of the lack of fit for Model i
T = temperature, K
t = time on stream, h
u = gas linear velocity, m h^{-1}
W = catalyst weight, g
$X^*_{i,j}$, $X_{i,j}$ = experimental and calculated value of composition of i lump for the j experimental condition
X_i = weight fraction of i component by mass unit of organic components
X_{i0} = weight fraction of i component at the reactor inlet by mass unit of organic components
$X_{i0}(\xi)$ = weight fraction of i component at zero time on stream at any dimensionless longitudinal position, ξ, in the reactor
X_W, X_{W0}, X_{Wf} = water/organic component ratio by mass, in the reaction medium, in the feed, and that formed, respectively
Z = total length of the reactor, m

Greek letters

α = confidence level
ε = bulk porosity
Φ = objective function
$(\nu_f)_i$ = degrees of freedom for the lack of fit for Model i
$\theta(X_W)$, $\theta_d(X_W)$ = functions for quantifying the effect of water in the reaction medium on the reaction rates for the steps in the kinetic scheme and on the kinetics of deactivation by coke
ρ = catalyst density, kg m^{-3}
ξ = dimensionless longitudinal coordinate of the reactor (z/Z)

Literature Cited

1. Demirbas A. Biofuels securing the planet's future energy needs. *Energy Conserv Manage*. 2009;50:2239–2249.
2. Nigam PS, Singh A. Production of liquid biofuels from renewable resources. *Prog Energy Comb Sci*. 2011;37:52–68.
3. Hahn-Hägerdal B, Galbe M, Gorwa-Grauslund MF, Lidén G, Zacchi G. Bio-ethanol—the fuel of tomorrow from the residues of today. *Trends Biotechnol*. 2006;24:549–556.
4. Park SH, Suh HK, Lee ChS. Effect ob bioethanol-biodiesel blending ratio on fuel spray behaviour and atomization characteristics. *Energy Fuels*. 2009;23:4092–4098.
5. Zhang W. Automotive fuels from biomass via gasification. *Fuel Process Technol*. 2010;91:866–876.
6. Gnansounou E. Production and use of lignocellulosic bioethanol in Europe: Current situation and perspectives. *Biores Technol*. 2010; 101:4842–4850.
7. Cardona CA, Sánchez OJ. Fuel ethanol production: Process design trends and integration opportunities. *Biores Technol*. 2007;98,2415–2457.
8. Hasegawa F, Yokoyama S, Imou K. Methanol or ethanol produced from woody biomass: Which is more advantageous? *Biores Technol*. 2010;101:109–111.
9. Chen H, Qiu W. Key technologies for bioethanol production from lignocellulose. *Biotechnol Adv*. 2010;28:556–562.
10. Ni M, Leung DYC, Leung MKH. A review on reforming bio-ethanol for hydrogen production. *Int J Hydrogen Energy*. 2007;32:3238–3247.
11. Sun J, Luo D, Xiao P, Jigang L, Yu, SH. High yield hydrogen production from low CO selectivity ethanol steam reforming over modified Ni/Y_2O_3 catalysts at low temperature for fuel cell application. *J Power Sources*. 2008;184:385–391.
12. Hernández L, Kafarov V. Use of bioethanol for sustainable electrical energy production. *Int J Hydrogen Energy*. 2009;34:7041–7050.
13. Inaba M, Murata K, Saito M, Takahara I. Ethanol conversion to aromatic hydrocarbons over several zeolite catalysts. *React Kinet Catal Lett*. 2006;88:135–142.
14. Széchényi A, Barthos R, Solymosi F. Aromatization of ethanol on Mo_2C/ZSM catalysts. *Catal Lett*. 2006;110:85–89.
15. Ren T, Patel MK, Blok K. Steam cracking and methane to olefins: Energy use, CO_2 emissions and production costs. *Energy*. 2008;33: 817–833.
16. Le Van Mao R, Levesque P, McLaughlin G, Dao LH. Ethylene from ethanol over zeolite catalysts. *Appl Catal*. 1987;34:163–179.
17. Le Van Mao R, Nguyen TM, McLaughlin GP. The bioethanol-to-ethylene (B.E.T.E.) process. *Appl Catal*. 1989;48:265–277.
18. Moser WR, Thompson W, Chiang Ch, Tong H. Silico-rich HZSM-5 catalyzed conversion of aqueous ethanol to ethylene. *J Catal*. 1989;117:19–32.
19. Le Van Mao R, Nguyen TM, Yao J. Conversion of ethanol in aqueous solution over ZSM-5 zeolites. Influence of reaction parameters and catalyst acidic properties as studied by ammonia TPD technique. *Appl Catal*. 1990;61:161–173.
20. Bi J, Guo X, Liu M, Wang X. High effective dehydration of bioethanol into ethylene over nanoscale HZSM-5 zeolite catalyts. *Catal Today*. 2010;149:143–147.
21. Schulz J, Bandermann F. Conversion of ethanol over zeolite H-ZSM-5. *Chem Eng Technol*. 1994;17:179–186.
22. Gayubo AG, Tarrio AM, Aguayo AT, Olazar M, Bilbao J. Kinetic modelling of the transformation of aqueous ethanol into hydrocarbons on a HZSM-5 zeolite. *Ind Eng Chem Res*. 2001;40:3467–3474.
23. Aguayo AT, Gayubo AG, Tarrio AM, Atutxa A, Bilbao J. Study of operating variables in the transformation of aqueous ethanol into hydrocarbons on a HZSM-5 zeolite. *J Chem Technol Biotechnol*. 2002;77:211–216.
24. Aguayo AT, Gayubo AG, Atutxa A, Olazar M, Bilbao J. Catalyst deactivation by coke in the transformation of aqueous ethanol into hydrocarbons. Kinetic modeling and acidity deterioration of the catalyst. *Ind Eng Chem Res*. 2002;41:4216–4224.
25. Gayubo AG, Alonso A, Valle B, Aguayo AT, Bilbao J. Selective production of olefins from bioethanol on HZSM-5 zeolite catalysts treated with NaOH. *Appl Catal B: Environ*. 2010;97:299–306.
26. Gayubo AG, Alonso A, Valle B, Aguayo AT, Bilbao J. Kinetic model for the transformation of bio-ethanol into olefins over a HZSM-5 zeolite treated with alkali. *Ind Eng Chem Res*. 2010;49:10836–10844.

27. Gayubo AG, Arandes JM, Olazar M, Aguayo AT, Bilbao J Calculation of the kinetics of deactivation by coke for a silica-alumina catalyst in the dehydration of 2-ethylhexanol. *Ind Eng Chem Res*. 1993;32:458–465.
28. Gayubo AG, Arandes JM, Aguayo AT, Olazar M, Bilbao J. Calculation of the kinetics of deactivation by coke in integral reactor for a triangular scheme reaction. *Chem Eng Sci*. 1993;48:1077–1087.
29. Gayubo AG, Arandes JM, Aguayo AT, Olazar M, Bilbao J. Contributions to the calculation of coke deactivation kinetics. Comparison of methods. *Chem Eng J*. 1994;55:125–134.
30. Gayubo AG, Aguayo AT, Alonso A, Bilbao J. Kinetic modelling of the MTO process on a SAPO-18 catalyst by considering deactivation and the formation of individual olefins. *Ind Eng Chem Res*. 2007;46:1981–1989.
31. Mokrani T, Scurrell M. Gas conversion to liquid fuels and chemicals: The methanol route-catalysis and processes development. *Catal Rev*. 2009;51:1–145.
32. Gayubo AG, Benito PL, Aguayo AT, Olazar M, Bilbao J. Relationship between surface acidity and activity of HZSM zeolite based catalysts in the MTG process. *J Chem Technol Biotechnol*. 1996;65:186–192.
33. Aguayo AT, Gayubo AG, Vivanco R, Olazar M, Bilbao J. Role of acidity and microporous structure in alternative catalysts for the transformation of methanol into olefins. *Appl Catal A: General*. 2005;283:197–207.
34. Phillips CB, Datta R. Production of ethylene from hydrous ethanol on H-ZSM-5 under mild conditions. *Ind Eng Chem Res*. 1997;36:4466–4475.
35. Aguayo AT, Gayubo AG, Ortega JM, Olazar M, Bilbao J. Catalyst deactivation by coke in the MTG process in fixed and fluidized beds reactors. *Catal Today*. 1997;37:239–248.
36. Gayubo AG, Aguayo AT, Morán AL, Olazar M, Bilbao J. Role of water in the kinetic modelling of catalyst deactivation in the MTG process. *AIChE J*. 2002;48:1561–1571.
37. Gayubo AG, Valle B, Aguayo AT, Olazar M, Bilbao J. Attenuation of catalyst deactivation by co-feeding methanol for enhancing the valorisation of crude bio-oil. *Energy Fuels*. 2009;23:4129–4136.
38. Bjorgen M, Svelle S, Joensen F, Nerlov J, Kolboe S, Bonino F, Palumbo L, Bordiga S, Olsbye U. Conversion of methanol to hydrocarbons over zeolite H-ZSM-5: On the origin of the olefinic species. *J Catal*. 2007;249:195–207.
39. Johansson R, Hruby SL, Rass-Hansen J, Christensen CH. The hydrocarbon pool in ethanol-to-gasoline over HZSM-5 Catalysts. *Catal Lett*. 2009;127:1–6.
40. Haw JF, Nicholas JB, Song W, Deng F, Wang Z, Xu T, Heneghan CS. Roles for cyclopentenyl cations in the synthesis of hydrocarbons from methanol on zeolite catalyst HZSM-5. *J Am Chem Soc*. 2000;122:4763–4775.
41. Seiler M, Wang W, Buchholz A. Direct evidence for a catalytically active role of the hydrocarbon pool formed on zeolite H-ZSM-5 during the methanol-to-olefin conversion. *Catal Lett*. 2003;88:187–191.
42. Wang W, Jiang YJ, Hunger M. Mechanistic investigations of the methanol-to-olefin (MTO) process on acidic zeolite catalysts by in situ solid-state NMR spectroscopy. *Catal Today*. 2006;113:102–114.
43. Tabak SA, Krambeck FJ, Garwood WE. Conversion of propylene and butylene over ZSM-5 catalyst. *AIChE J*. 1986;32:1526–1531.
44. Guisnet M, Magnoux P. Organic chemistry of coke formation. *Appl Catal A: General*. 2001;212:83–96.
45. Guisnet M, Costa L, Ramôa Ribeiro F. Prevention of zeolite deactivation by coking. *J Mol Catal A: Chem*. 2009;305:69–83.
46. Ferreira Madeira F, Gnep NS, Magnoux P, Vezin H, Maury S, Cadran N. Mechanistic insights on the ethanol transformation into hydrocarbons over HZSM-5 zeolite. *Chem Eng J*. 2010;161:403–408.
47. Kim J, Choi M, Ryoo R. Effect of mesoporosity against the deactivation of MFI zeolite catalyst during the methanol-to-hydrocarbon conversion process. *J Catal*. 2010;269:219–228.

Manuscript received Dec. 10, 2010, and revision received Feb. 15, 2011.